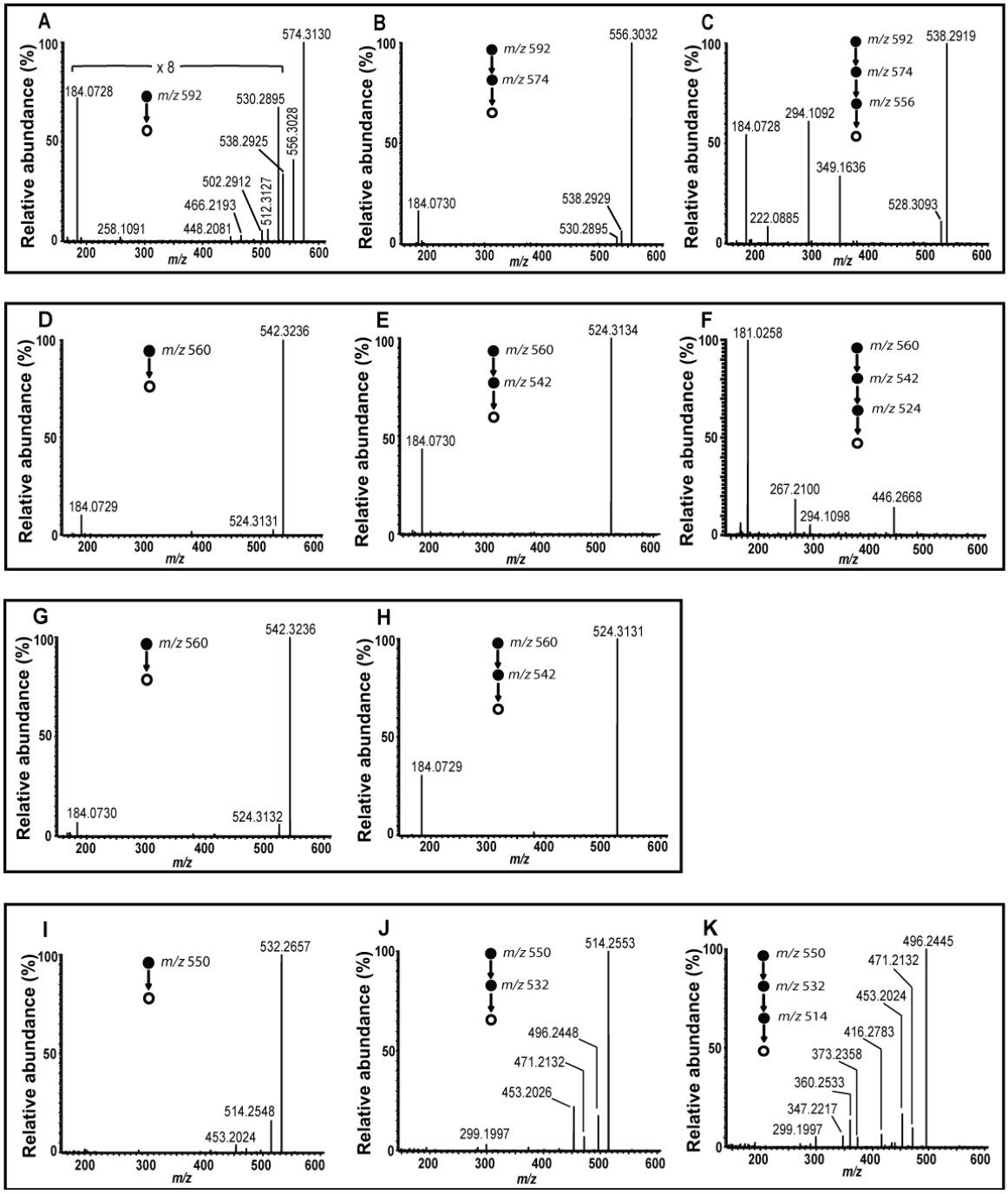

Figure S1, Related to Figure 1. High mass resolution and high mass accuracy multistage tandem mass spectra MS^n. Multiple stage MS^n (n=2-4) experiments were performed in the LTQ ion trap and the resultant fragmentation ions were detected in an Orbitrap instrument with a mass resolution of 30,000 at *m/z*=400 and a mass accuracy within 5 ppm. The first panel from the top (corresponding PGE_2-LPC): **A**, The MS^2 spectrum of the parent M^+ ions at *m/z* 592; **B**, the resultant MS^3 spectrum of the fragment ions derived from the ion at *m/z* 574 (592 → 574); **C**, the resultant MS^4 spectrum of the ion at *m/z* 556 (592 → 574 → 556). The second panel from the top (corresponding to 11-HETE-LPC): **D**, The MS^2 spectrum of the parent M^+ ion at *m/z* 560; **E**, the resultant MS^3 spectrum of the fragment ions at *m/z* 542 (560 → 542); **F**, the resultant MS^4 spectrum of the ions at *m/z* 524 (560 → 542 → 524). The third panel from the top (corresponding 15-HETE-LPC): **G**, The MS^2 spectrum of the parent M^+ ion at *m/z* 560; **H**, the resultant MS^3 spectrum of the fragment ions at *m/z* 542 (560 → 542). The bottom panel (corresponding PGE_2-LPE): **I**, The MS^2 spectrum of the parent M^+ ions at *m/z* 550; **J**, the resultant MS^3 spectrum of the fragment ions derived from the ion at *m/z* 532 (550 → 532); **K**, the resultant MS^4 spectrum of the ion at *m/z* 514 (550 → 532 → 514).

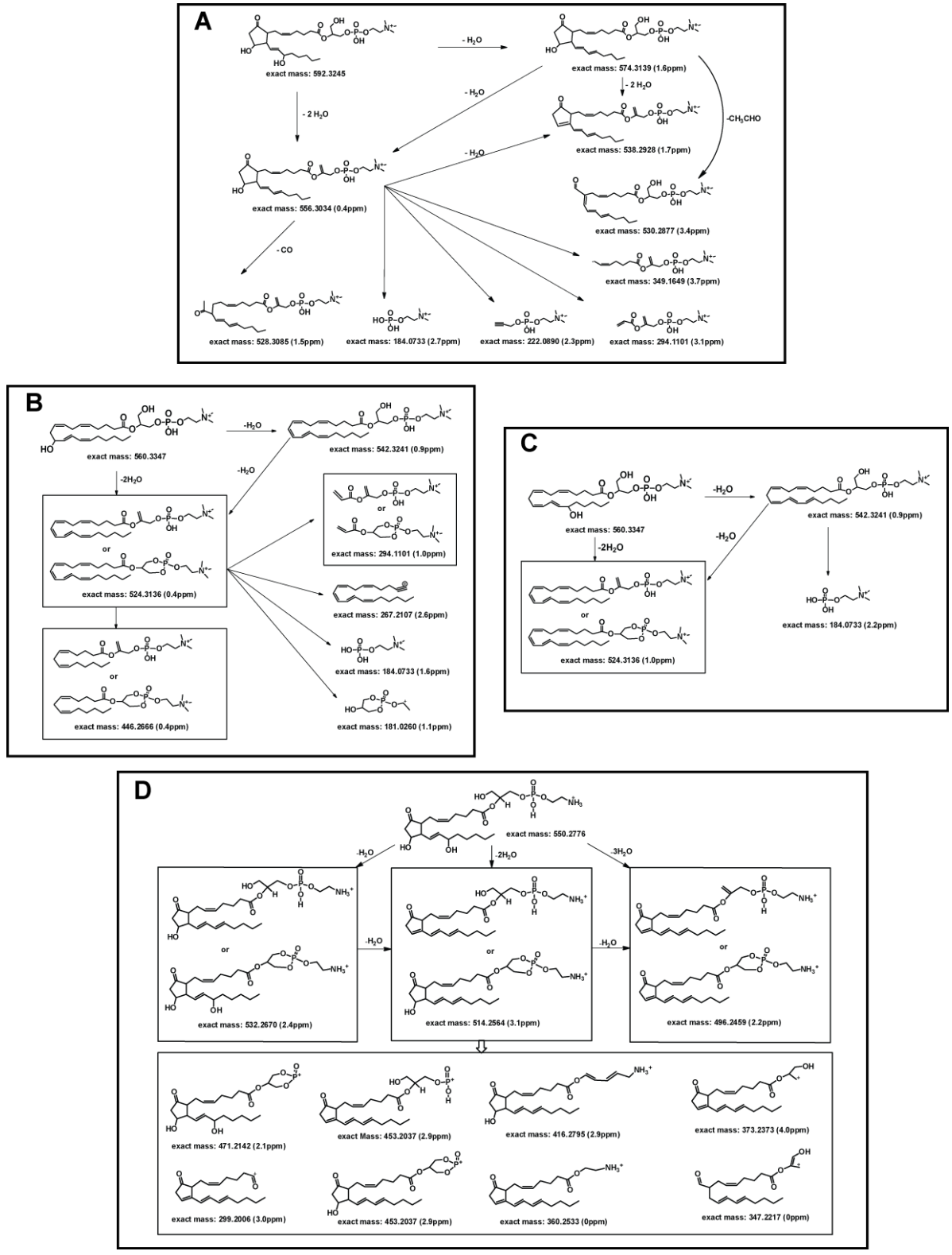

Figure S2, **Related to Figure 1 and Figure S1**. Proposed fragmentation pathways for eicosanoid-lysolipids: PGE_2-LPC (**A**); 11-HETE-LPC (**B**); 15-HETE-LPC (**C**); and PGE_2-LPE (**D**). Exact masses are calculated theoretical masses, numbers in parentheses indicate the measured mass error in parts per million (ppm) relative to the calculated theoretical mass.

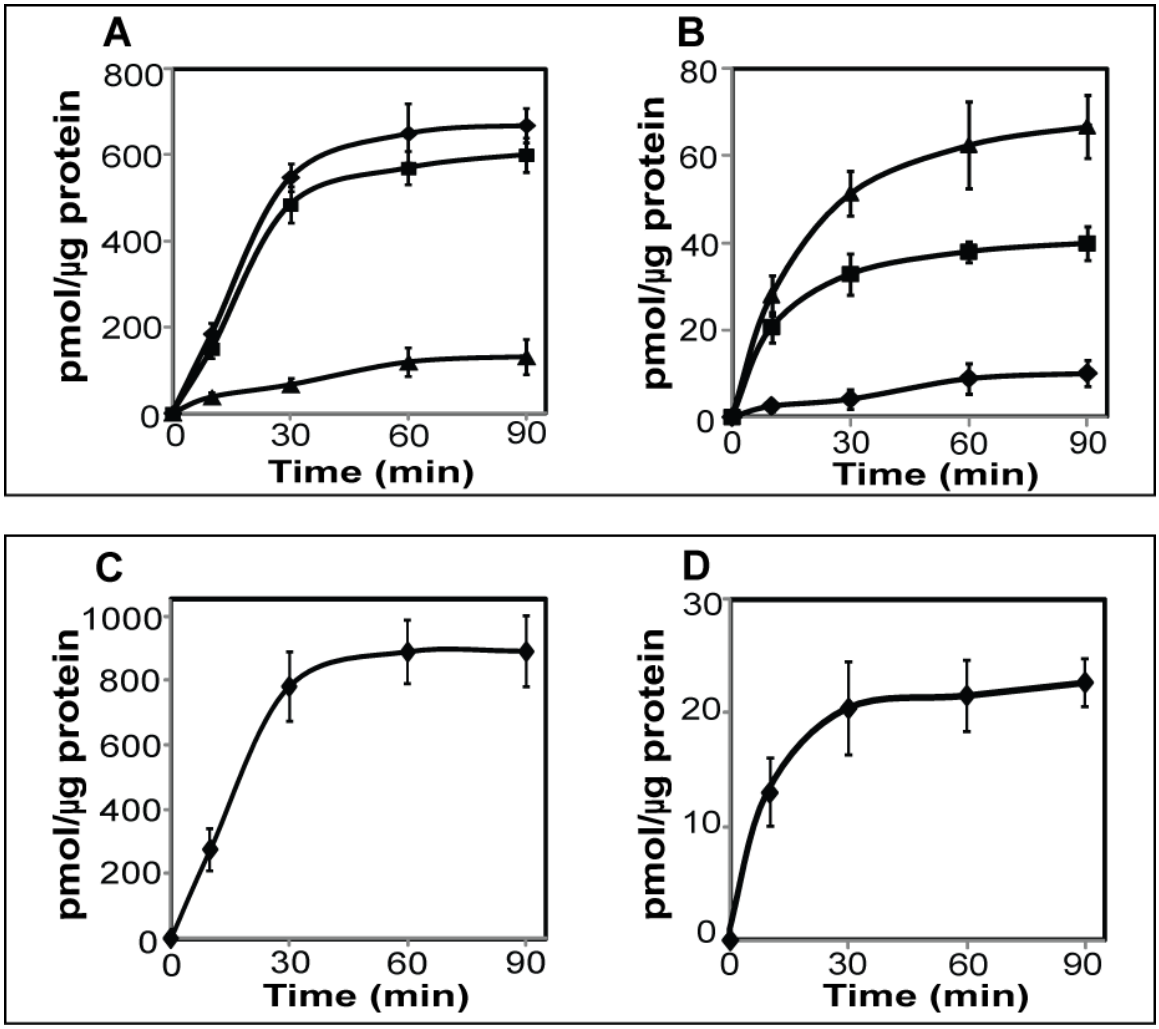

Figure S3, Related to Figure 1A and Figure 1B. COX-2 mediated oxidation of 2-AA-LPC and 2-AA-LPE is inhibited by aspirin. Purified recombinant COX-2 or aspirin acetylated COX-2 was incubated with either 2-AA-LPC (10 µM) or 2-AA-LPE (10 µM) at 30 °C for indicated times. The reaction was then terminated, extracted using solid phase extraction and analyzed by LC-MS. **A,** Time course of COX-2 mediated oxidation of 2-AA-LPC (◆ PGE_2-LPC; ■ 11-HETE-LPC; ▲ 15-HETE-LPC); **B,** Inhibition of COX-2 mediated generation of eicosanoid-LPC molecular species by aspirin (◆ PGE_2-LPC; ■ 11-HETE-LPC; ▲ 15-HETE-LPC); **C,** Time course of COX-2 mediated oxidation of 2-AA-LPE (◆ PGE_2-LPE); **D,** Inhibition of COX-2 mediated generation of PGE_2-LPE by aspirin (◆ PGE_2-LPE). Data are expressed as mean values ± SEM of three replicates.

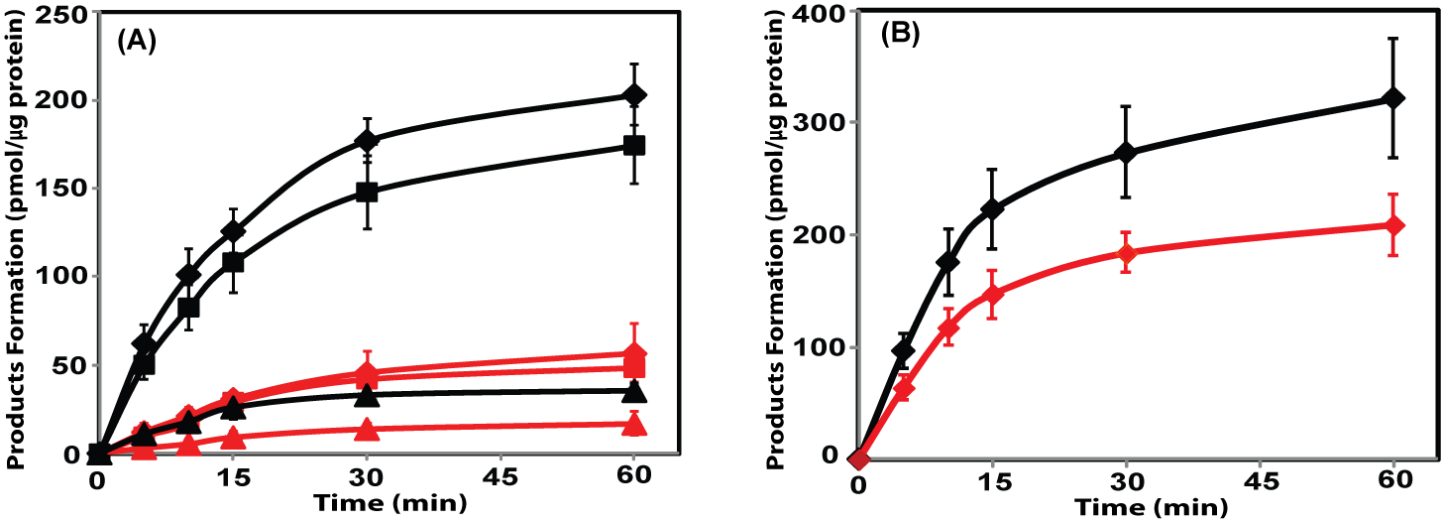

Figure S4, Related to Figure 1A and Figure 1B. Increased production of oxidized 2-AA-LPC and 2-AA-LPE by COX-2 utilizing large unilamellar vesicles (LUVs) in comparison to small unilamellar vesicles (SUVs). 2-AA-LPC (10 µM) (**A**) or 2-AA-LPE (10 µM) (**B**) present in SUVs (red) or LUVs (black) comprised of DOPC (70 µM) and DOPE (20 µM) were incubated with COX-2 for the indicated times as described in "Supplemental Experimental Procedures". The reaction was then terminated, extracted and analyzed by LC-MS. Data are expressed as mean values ± SEM of three independent replicates. **A:** Oxidation of 2-AA-LPC incorporated into LUVs (black) or SUVs (red) by COX-2: ◆ PGE_2-LPC; ■ 11-HETE-LPC; ▲ 15-HETE-LPC; **B:** Oxidation of 2-AA-LPE incorporated into LUVs (black) or SUVs (red) by COX-2: ◆ PGE_2-LPE.

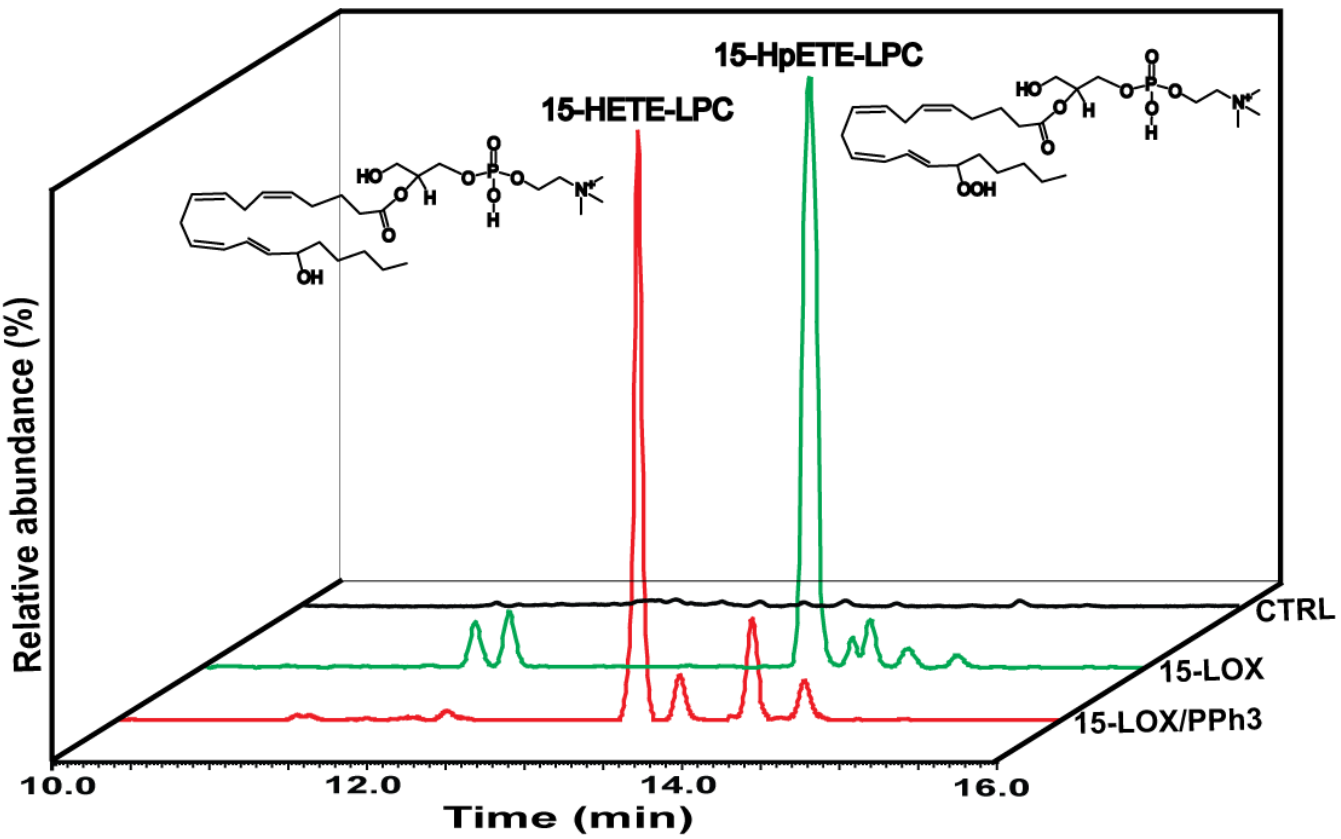

Figure S5, Related to Figure 5. Extracted ion chromatograms (with 3 ppm mass window) of 15-HpETE-LPC (m/z 576.3296) and 15-HETE-LPC (m/z 560.3347) generated from 15-lipoxygenase mediated oxidation of 2-AA-LPC. 2-AA-LPC (10 μM) in 50 mM Tris-HCl buffer (pH 7.4) was incubated with/without (CTRL) purified recombinant 15-LOX (2 μg) at 37°C for 10 min. The reaction was terminated by addition of methanol and acidified to pH 4 with glacial acetic acid. The reaction products were then purified by solid phase extraction following separation on a C18 HPLC column prior to analysis utilizing an LTQ-Orbitrap mass spectrometer with a mass resolution of 30,000 at *m/z* 400 Th in the positive ion mode. Chemical structures of the identified metabolic products 15-HpETE-LPC and 15-HETE are shown.

Table S1, **Related to Figure 1**. Chemical formula and accurate mass of 2-AA-LPC and 2-AA-LPE plus the addition of 1 to 6 oxygen atoms with varying degrees of unsaturation in the acyl chain.

Chemical Formula	Accurate Mass	Chemical Formula	Accurate Mass
$C_{28}H_{51}NO_7P^+$	544.3398	$C_{25}H_{45}NO_7P^+$	502.2928
$C_{28}H_{51}NO_8P^+$	560.3347	$C_{25}H_{45}NO_8P^+$	518.2877
$C_{28}H_{49}NO_8P^+$	558.3190	$C_{25}H_{43}NO_8P^+$	516.2721
$C_{28}H_{51}NO_9P^+$	576.3296	$C_{25}H_{45}NO_9P^+$	534.2826
$C_{28}H_{49}NO_9P^+$	574.3139	$C_{25}H_{43}NO_9P^+$	532.2670
$C_{28}H_{47}NO_9P^+$	572.2983	$C_{25}H_{41}NO_9P^+$	530.2513
$C_{28}H_{51}NO_{10}P^+$	592.3245	$C_{25}H_{45}NO_{10}P^+$	550.2726
$C_{28}H_{49}NO_{10}P^+$	590.3089	$C_{25}H_{43}NO_{10}P^+$	548.2619
$C_{28}H_{47}NO_{10}P^+$	588.2932	$C_{25}H_{41}NO_{10}P^+$	546.2463
$C_{28}H_{51}NO_{11}P^+$	608.3194	$C_{25}H_{45}NO_{11}P^+$	566.2725
$C_{28}H_{49}NO_{11}P^+$	606.3194	$C_{25}H_{43}NO_{11}P^+$	564.2568
$C_{28}H_{47}NO_{11}P^+$	604.2881	$C_{25}H_{41}NO_{11}P^+$	562.2412
$C_{28}H_{51}NO_{12}P^+$	624.3143	$C_{25}H_{45}NO_{12}P^+$	582.2674
$C_{28}H_{49}NO_{12}P^+$	622.2987	$C_{25}H_{43}NO_{12}P^+$	580.2517
$C_{28}H_{47}NO_{12}P^+$	620.2830	$C_{25}H_{41}NO_{12}P^+$	578.2361
$C_{28}H_{51}NO_{13}P^+$	640.3093	$C_{25}H_{45}NO_{13}P^+$	598.2623
$C_{28}H_{49}NO_{13}P^+$	638.2936	$C_{25}H_{43}NO_{13}P^+$	596.2467
$C_{28}H_{47}NO_{13}P^+$	636.2780	$C_{25}H_{41}NO_{13}P^+$	594.2310
$C_{28}H_{45}NO_{13}P^+$	634.2623	$C_{25}H_{39}NO_{13}P^+$	592.2154
$C_{28}H_{43}NO_{13}P^+$	632.2467	$C_{25}H_{37}NO_{13}P^+$	590.1997

Table S2, Related to Figure 1 and Figure S5. Measured K_m values for various products formed from oxidation of 2-AA-LPC and 2-AA-LPE in comparison to other substrates.

Enzyme	Substrate	Product	K_m (μM)	Comparison to different substrates
COX-2	2-AA-LPC	PGE_2-LPC	11.7 (±2.3)	K_m = 6.5 μM[a]
COX-2	2-AA-LPC	11-HETE-LPC	12.3 (±2.7)	K_m = 1-15 μM[b]
COX-2	2-AA-LPC	15-HETE-LPC	30.0 (± 9.3)	K_m = 4.4 (± 0.9) μM[c]
COX-2	2-AA-LPE	PGE_2-LPE	8.2 (±2.3)	K_m = 1.9 (± 0.37) μM[d]
15-LOX	2-AA-LPC	15-HpETE-LPC	7.5 (±1.8)	K_m = 13 (± 4) μM[e]
				K_m = 7 (± 2) μM[f]

[a,b]K_m values for oxidation of arachidonic acid by COX-2 (Smith et al., 2000; Smith et al., 2011); [c]K_m value for oxidation of 2-arachidonylglycerol by COX-2 (Kozak et al., 2000); [d,e]K_m values for oxidation of arachidonic acid by15-LOX (Kozak et al., 2002; Kobe et al., 2014); [f]K_m values for oxidation of 2-arachidonylglycerol by15-LOX (Kozak et al., 2002).

Table S3, Related to Figure 4 and Figure 6. The levels of PGE_2, 11-HETE and 15-HETE eicosanoids in murine hepatic tissue and in human myocardium. Data are expressed as mean values ± SEM of six replicates.

Tissue Type	PGE_2 (pg/mg tissue)	11-HETE (pg/mg tissue)	15-HETE (pg/mg tissue)
Wild-type Mouse Liver	1.9 (± 0.7)	9.6 (± 1.3)	16.6 (± 2.4)
$iPLA_2\gamma^{-/-}$ Mouse Liver	1.2 (± 0.3)	5.2 (± 0.8)	6.8 (± 0.8)
Human Heart	2.4 (± 0.3)	2.2 (± 0.2)	3.8 (± 1.2)

SUPPLEMENTAL EXPERIMENTAL PROCEDURES

Materials. The following chemicals were purchased from Cayman Chemical (Ann Arbor, MI): 9-oxo-11*R*,15*S*-dihydroxy-5*Z*,13*E*-prostadienoic acid (PGE_2), PGE_2-d4, 9-oxo-11*R*,15*R*-dihydroxy-5Z,13E-prostadienoic acid (15(*R*)-PGE_2), 9-oxo-11*R*,15*S*-dihydroxy-5Z,13E-prostadienoic acid-cyclo[8*S*,12*R*] (8-iso-PGE_2), 9-oxo-11*S*,15*S*-dihydroxy-5Z,13E-prostadienoic acid (11β-PGE_2), 11-hydroxy-5Z,8Z,12E,14Z-eicosatetraenoic acid (11-HETE), 12-hydroxy-5Z,8Z,10E,14Z-eicosatetraenoic acid (12-HETE)-d8, 11(*R*)-hydroxy-5Z,8Z,12E,14Z-eicosatetraenoic acid (11(*R*)-HETE), 15-hydroxy-5Z,8Z,11Z,13E-eicosatetraenoic acid (15-HETE), 15(*S*)-hydroxy-5Z,8Z,11Z,13E-eicosatetraenoic acid (15(*S*)-HETE), 2-(acetyloxy)-benzoic acid (aspirin), N-(4-aminomethylphenyl)-pyridinium (AMPP), human recombinant cyclooxygenase-2 (COX-2), ovine cyclooxygenase-1 (COX-1), and human recombinant 15-lipoxygenase-2 (15-LOX). Cytosolic phospholipase $A_2\alpha$ ($cPLA_2\alpha$) containing a C-terminal $(His)_6$ tag was expressed in Sf9 cells utilizing a Bac-to-Bac® recombinant baculovirus system from Thermo-Fisher Scientific (Waltham, MA) and purified using sequential Co^{2+} HIS-select affinity and MonoQ FPLC chromatographies (Yan et al., 2005). HPLC-grade acetonitrile, methanol, chloroform, and water were purchased from Burdick & Jackson (Muskegon, MI). Glacial acetic acid and N, N-dimethylformamide were obtained from Sigma-Aldrich (St Louis, MO). N-hydroxybenzotriazole and 3-(dimethylamino)propyl)-ethyl carbodiimide hydrochloride were purchased from Advanced Chem Tech (Louisville, KY) and TCI America (Portland, OR), respectively. Ascentis Express C18 reverse phase high performance liquid chromatography (HPLC) columns (15cm x 2.1mm) were obtained from Supelco (Bellefonte, PA), Chiralpak® AD-RH chiral phase HPLC columns (15 cm x 2.1 mm) were purchased from Chiral Technologies Inc. (West Chester, PA), and solid phase extraction Strata-X columns were purchased from Phenomenex (Torrance, CA). 2-Arachidonoyl-lysophosphatidylethanolamine (2-AA-LPE) was synthesized by acid hydrolysis of 1-O-1'-(Z)-octadecenyl-2-arachidonoyl-*sn*-glycero-3-phosphoethanolamine and purified by RP-HPLC; 2-Arachidonoyl-lysophosphatidylcholine (2-AA-LPC) was prepared, purified and quantified as described previously (Creer and Gross, 1985; Creer et al., 1985).

Reverse phase liquid chromatography-tandem mass spectrometry ($LC\text{-}MS^n$). $LC\text{-}MS^n$ analyses were performed using an LTQ-Orbitrap mass spectrometer (Thermo Scientific, San Jose, CA) equipped with a Surveyor HPLC system (Thermo Scientific, San Jose, CA). Briefly, solid phase extractions of the cyclooxygenase reaction mixtures utilizing 2-AA-LPC or 2-AA-LPE as substrate were separated on a C18 reverse phase column (Ascentis Express, 2.7 μm particles, 150× 2.1 mm) at 23°C using a linear gradient of solvent A (0.1% glacial acetic acid in water) and solvent B (0.1% glacial acetic acid in acetonitrile) at a flow rate of 0.2 ml/min. The following solvent gradient program was used: 0.0-5.0 min, 25% B; 5.0-7.0 min, 25-35% B; 7.0-20.0 min, 35-60% B; 20.0-20.1 min, 60-100% B; 20.1-28.0 min, 100% B; 28.0-28.1 min, 100% B to 25% B followed by 10 min isocratic re-equilibration at 25% B. The sample injection volume was 10 μl and the autosampler tray temperature was kept at 4°C throughout the analysis. Mass spectrometric analyses were performed using an LTQ-Orbitrap mass spectrometer. The LTQ ion source was operated in the positive ion mode at sheath, auxiliary, and sweep gas flows (arbitrary units) of 40, 5, and 1, respectively. The capillary temperature was set to 275°C, and the electrospray voltage was 4.1 kV. Capillary voltage and tube lens voltage were set at 30V and 110V, respectively. The mass spectrometer was calibrated using the manufacturer's recommended positive mode calibration solution containing L-methionyl-arginyl-phenylalanyl-alanine acetate, Ultramark 1621, and caffeine. Resolving powers (at *m/z* 400 Th) of 30,000 in full scan mode and in MS/MS mode were used. The mass accuracy was within 5 ppm at mass values from *m/z* 130 to 2000. For MS/MS analyses, a normalized collision energy of 30% was applied and the activation time was set at 30 ms with an activation parameter of q = 0.25. Data acquisition was performed using an Xcalibur operating system, version 2.1 (Thermo Scientific).

Chiral phase liquid chromatography-tandem mass spectrometry. Chiral phase $LC\text{-}MS^n$ analyses were performed similarly to those employing reverse phase liquid chromatography using an LTQ-Orbitrap mass spectrometer as described above. The AMPP derivatized eicosanoids were injected and separated on a Chiralpak® AD-RH chiral phase HPLC column (5.0 μm particles, 150 mm× 2.1 mm) at 23°C using a linear gradient of solvent A (0.1% glacial acetic acid in water) and solvent B (0.1% glacial acetic acid in acetonitrile) at a flow rate of 0.2 ml/min. The following solvent gradient program was used: 0.0-1.0 min, 5-22% B; 1.0-7.0 min, 22-26% B; 7.0-7.1 min, 26-40% B; 7.1-20.0 min, 40-60% B; 20.0-21.0 min, 60-100% B; 21.0-29.0 min, 100% B prior to isocratic re-equilibration at 5% B for 10 min. The sample injection volume was 10 μl and the autosampler tray temperature was kept at 4°C throughout the analysis. Mass spectrometric analysis conditions were the same as described above in the section "Reverse Phase Liquid Chromatography-Tandem Mass Spectrometry".

COX-2 mediated oxidation of 2-AA-LPC and 2-AA-LPE present as guest in small unilamellar vesicles (SUVs) or large unilamellar vesicles (LUVs). SUVs comprised of 1,2-dioleoyl-*sn*-glycero-3-phosphocholine **(**DOPC) / 1,2-dioleoyl-sn-glycero-3-phosphoethanolamine **(**DOPE) / 2-AA-LPC (35 nmol/10 nmol/5 nmol) or DOPC/DOPE/2-AA-LPE (35 nmol/10 nmol/5 nmol) were prepared by sonication at 30% power using a 1s duty cycle in the presence of 500 μl of 100 mM Tris-HCl buffer (pH 8.0) containing 10% glycerol. LUVs of identical lipid compositions were prepared by extrusion through a polycarbonate membrane (0.8 μm pore size, 15 passages through the membrane) using a Mini-Extruder (Avanti). Purified COX-2 was then incubated with the above vesicle preparations at 30°C for the indicated times. After addition of 80 μl methanol, the mixture was acidified to pH 4 with glacial acetic acid. The eicosanoids-lysolipids were then extracted by solid phase extraction and analyzed by reverse phase LC-MS as described above.

Human myocardium and murine hepatic tissue sample preparation and analysis of eicosanoids and eicosanoid-lysolipids. Murine hepatic tissue from either control C57BL/6 mice or $iPLA_2\gamma^{-/-}$ mice (12-14 weeks male mice, prepared as we previously described (Mancuso et al., 2007; Mancuso et al., 2009; Mancuso et al., 2010)) or human myocardium were analyzed for eicosanoid-lysolipid content after rapid removal and flash-freezing in liquid nitrogen and stored at -180ºC until homogenization. Samples were homogenized and extracted using a modified Bligh and Dyer procedure. Briefly, ~80 mg of tissue was extracted by addition of 3 ml of ice-cold $CH_3OH/CHCl_3$ (1:2 v/v containing 2% glacial acetic acid) followed directly by addition of 17:0-LPC as an internal standard. Next, the samples were homogenized using a polytron homogenizer at 0-4°C and 1 ml of ice-cold H_2O was added prior to separation

of the organic and aqueous phases by centrifugation at 15,000g for 15 min. The $CHCl_3$ layer was transferred to a new tube while the aqueous layer was re-extracted by subsequent addition of 2 ml $CHCl_3$, vortexing, and phase separation by centrifugation at 15,000g for 15 min. The $CHCl_3$ extracts were combined, evaporated under a nitrogen stream and resuspended in 100 µl of 80% methanol in water prior to LC-MS/MS analyses as described above. Eicosanoid analyses were performed using the methods we previously described (Liu et al., 2013).

Statistical Analysis. Statistical analysis was performed using the two-tailed Student's *t* test. *P* values of less than 0.05 were considered to be statistically significant. All data are reported as the mean ±SEM unless otherwise noted.

SUPPLEMENTAL REFERENCES

Creer, M.H., Pastor, C., Corr, P.B., Gross, R.W., and Sobel, B.E. (1985). Quantification of choline and ethanolamine phospholipids in rabbit myocardium. Anal. Biochem. *144*, 65-74.

Creer, M.H., and Gross, R.W. (1985). Separation of isomeric lysophospholipids by reverse phase HPLC. Lipids 20, 922-928.

Kobe, M.J., Neau, D.B., Mitchell, C.E., Bartlett, S.G., and Newcomer, M.E. (2014). The Structure of Human 15-Lipoxygenase-2 with a Substrate Mimic. J. Biol. Chem. *289*, 8562–8569.

Kozak, K.R., Gupta, R.A., Moody, J.S., Ji, C., Boeglin, W.E., DuBois, R.N., Brash, A.R., and Marnett, L.J. (2002).15-Lipoxygenase Metabolism of 2-Arachidonylglycerol. J. Biol. Chem. *277*, 23278–23286.

Kozak, K.R., Rowlinson, S.W., and Marnett, L.J. (2000). Oxygenation of the endocannabinoid, 2-arachidonylglycerol, to glyceryl prostaglandins by cyclooxygenase-2. J. Biol. Chem. *275*, 33744-33749.

Liu, X., Moon, S.H., Mancuso, D.J., Jenkins, C.M., Guan, S., Sims, H.F., and Gross, R.W. (2013). Oxidized fatty acid analysis by charge switch derivatization, selected reaction monitoring, and accurate mass quantitation. Anal. Biochem. *442*, 40-50.

Smith, T., Leipprandt, J., and DeWitt, D. (2000). Purification and Characterization of the Human Recombinant Histidine-Tagged Prostaglandin Endoperoxide H Synthases-1 and -2. Arch. Biochem. Biophys. *375*, 195-200.

Smith, W.L., Urade, Y., and Jakobsson, P.J. (2011). Enzymes of the Cyclooxygenase Pathways of Prostanoid Biosynthesis. Chem. Rev. *111*, 5821–5865.

Yan, W., Jenkins, C.M., Han, X., Mancuso, D.J., Sims, H.F., Yang, K., and Gross, R.W. (2005). The Highly Selective Production of 2-Arachidonoyl Lysophosphatidylcholine Catalyzed by Purified Calcium-independent Phospholipase $A_2\gamma$. J. Biol. Chem. *280*, 26669-26679.

Mancuso, D.J., Sims, H.F., Yang, K., Kiebish, M.A., Su, X., Jenkins, C.M., Guan, S., Moon, S.H., Pietka, T., Nassir, F. et al. (2010). Genetic ablation of calcium-independent phospholipase $A_2\gamma$ prevents obesity and insulin resistance during high fat feeding by mitochondrial uncoupling and increased adipocyte fatty acid oxidation. J. Biol. Chem. *285*, 36495-36510.

Mancuso, D.J., Kotzbauer, P., Wozniak, D.F., Sims, H.F., Jenkins, C.M., Guan, S., Han, X., Yang, K., Sun, G., Malik, I. et al. (2009). Genetic ablation of calcium-independent phospholipase $A_2\gamma$ leads to alterations in hippocampal cardiolipin content and molecular species distribution, mitochondrial degeneration, autophagy, and cognitive dysfunction. J. Biol. Chem. *284*, 35632-35644.

Mancuso, D.J., Sims, H.F., Han, X., Jenkins, C.M., Guan, S.P., Yang, K., Moon, S.H., Pietka, T., Abumrad, N.A., Schlesinger, P.H. et al. (2007). Genetic ablation of calcium-independent phospholipase $A_2\gamma$ leads to alterations in mitochondrial lipid metabolism and function resulting in a deficient mitochondrial bioenergetic phenotype. J. Biol. Chem. *282*, 34611-34622.